

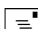
Development of Naturally-Derived Biomaterials and Optimization of Their Biomechanical Properties

J.C. Coburn and A. Pandit

Summary

Since surgeons have endeavored to repair the human body, there has been a need for materials to suit that purpose. Not surprisingly, many of the first materials used for these procedures were of natural sources either xenogenic or allogenic. When synthetic materials became more prevalent in the early 20th century, a huge market for synthetic implants was realized. The advantages, and disadvantages, of using naturally-derived biomaterials were known only in general terms and the ensuing decades saw only a modest increase in usage of these materials. Not until the recent times, have naturally-derived biomaterials been explored as facilitators and promoters of healing and regeneration. Today, biomaterials of all types are being used for everything from wound dressing to tendon and ligament repair. Extensive experimentation has been undertaken to identify the composition, mechanical properties, and in vivo response of naturally-derived biomaterials. In this review, we present a brief history of naturally-derived biomaterials, their recent applications, and methods of characterization. Methods to optimize the morphological and mechanical properties of such a biomaterial for individual applications are then discussed in detail.

Keywords. Natural biomaterials, mechanical properties, extracellular matrix

 *Correspondence to: A.Pandit, Department of Mechanical and Biomedical Engineering, National University of Ireland, Galway, Galway, Ireland. Phone: +353 91 492758. Fax: +353 91 563991. E-mail: abhay.pandit@nuigalway.ie.

Introduction

The surgeon has, at their disposal, a myriad of choices of biomaterials, for a plethora of surgical procedures including sutures, artificial heart valves, wound dressings, and total joint replacements to name just a few. The definitions of a biomaterial cover an equally broad spectrum. In a very general sense: “Biomaterials are materials (synthetic and natural; solid and sometimes liquid) that are used in medical devices or in contact with biological systems”(1). The choice of biomaterial depends on the type of procedure being performed (Table 1), the severity of the patient’s condition, and the surgeon’s preference. To be successful, the implant should effectively repair the defect it covers without eliciting an adverse tissue reaction while maintaining mechanical and biological integrity for a desired amount of time from a few weeks to several years.

The prime reason biomaterials have come about is to provide a remedy for surgical problems. In the beginning, a physician was able to try almost anything if they thought it would help their patient survive and recover from their ailment. If the part fit, they could implant it. Though early physicians lacked the sophistication and technology of modern surgeons, some were able to intuitively grasp concepts of biomimicry necessary to successfully plan these operations. Of course, without knowledge of the immunogenicity of the implants they were using, many patients experienced complications or died soon after surgery. Today, the field has advanced to where most biomedical materials research is being done outside of the operating room and in the laboratory. Surgeons routinely use approved biomaterials for hundreds of types of procedures, creating a multi-million dollar market (Table 1).

Prostheses made from naturally-derived biomaterials are frequently the decellularized extracellular matrix (ECM) of an animal (xenograft) or human (allograft). There are several advantages to using ECM biomaterials is. First, all the molecules in an ECM can be broken down by normal enzymatic processes. Second, the three-dimensional structure and morphology of the ECM resembles the structure and morphology of the native tissue that is being replaced. Lastly, because of the nature of the biomaterial, researchers can design a prosthesis that works not only on a macroscopic level, but also on the cellular level. Along with the advantages, there are certainly some disadvantages as well. ECMs are frequently immunogenic, causing harsh reactions in the host. There are also many ancillary molecules that change the way the prosthetic will interact when placed *in vivo*. Some molecules can enhance the regenerative capabilities of

the surrounding tissue while others provoke an immune response (2). All told, there is a wealth of potential in ECM biomaterials as well as concerns that need to be addressed. Navigating them is the job of biomaterials researchers.

We will confine our discussion to the development and optimization of the mechanical properties of ECM biomaterials. First, we present a brief history of ECM biomaterials, their recent applications, and methods of characterization. Then we look more deeply into methods to optimize the mechanical properties of such a biomaterial for individual applications.

Table 1. Healthcare market and biomaterials usage in the United States.

Total US health expenditures (2003) ¹	\$1,678.9 billion
Percent of GDP ²	15 percent
Number of employees ²	10 million
Total Medical device market (2006 estimated) ³	\$86 billion
Number of employees in medical device industry ⁴	441,400
Medical device sales (2000) ⁵	\$44 billion
Biocompatible materials (2007) ⁶	\$22.2 billion
Implantable medical devices (2006) ⁶	\$7.9 billion
Tissue replacements (2006) ⁶	\$11.7 billion
Skin repair (projected 2007) ⁷	\$270 million
Vascular grafts (2000) ⁵	\$650,000
Number of devices (1990) ⁸	
Intraocular lenses	1,400,000
Contact lenses	4,000,000
Heart valves	45,000
Artificial knees	816,000
Artificial hips	521,000

¹Espicom: 2006, ²World Health Organization: 2006, ³Advamed: 2006, ⁴Medical Product Outsourcing: 2006,

⁵McMaster University: 2006, ⁶BCC Research: 2006-7, ⁷International Access Corporation: 2002, ⁸Ratner *et al.*[1]

A brief history

The new interest in natural biomaterials could really be classified as a renaissance. Historians have traced the use of sutures made from animal sinew to ancient Egypt. Some say, they were used even earlier. As early as the first century AD in both Greece and India, physicians were using natural biomaterials while performing plastic surgery to repair mutilations from battle and punishment. There are even accounts of physicians treating disemboweled soldiers to good effect

(3). One of the more interesting cases of this time period comes from India, recorded in a medical encyclopedia by Sushruta. It describes a procedure where physicians were able to create a prosthetic nose for patients whose nose was cut off. This procedure used a skin graft from the patient's cheek to mold the new prosthetic nose (3). This accomplishment occurred two thousand years ago, before aseptic technique, precision instruments, or the understanding of body cellular mechanics. Physicians were able to keep an open wound at the nose clean and viable, detach a portion patient's skin while maintaining the blood supply so it did not undergo necrosis, and finally reattach it to the patient so that it revascularized and the new nose sustained itself. Sushruta's record may be the first documented case of a prosthetic autograft, an easy to use, natural biomaterial.

Due to cultural, religious, and political unrest through the ages, knowledge of many aspects of medicine were lost until the Renaissance saw a reawakening of the process of scientific inquiry. A rhinoplasty similar to the one performed in 1st century India, using the skin of the arm, was recorded circa 1460 (3). Two hundred years later, in the 1660s, two of the first xenografts were reportedly performed in France and the Netherlands. In France in 1667, reports state that Jean-Baptiste Denis transfused blood from a lamb into a human and the patient survived. He did this several subsequent times, but mediocre results led to the procedure being banned in France (4). In Amsterdam, JJ van Meekeren gives an account of the repair of a cranial defect in a Russian nobleman using a piece adapted from the skull of a recently deceased dog. Unfortunately, the catholic church saw the implantation of a piece of an animal into the head of a Christian man as a desecration of the body and excommunicated the patient (5). Though these attempts to advance medicine were met with a cold reception from the political entities of the day, they set the stage for continued attempts. Implant technology progressed slowly until aseptic technique, anesthesia, and a basic understanding of cellular-level mechanisms matured.

Dental implants did not experience many of the problems that plagued more invasive implants and therefore were able to be developed during the 19th century. During that period, dentists began fabricating and placing implants from gold and platinum (6). It was not until the early 20th century however, that development of synthetic implants took off. One of the fathers of the field was an orthopedic surgeon named M.N. Smith-Petersen. In 1923, when he saw a piece of glass removed from a patient that had been successfully encapsulated by the body. This gave rise to the idea that these types of inert materials could be used in arthroplasty. That same

year, he constructed the first glass mould arthroplasty. These moulds performed reasonably well, but were prone to breakage after several months (7). The design was revised several times using materials such as a celluloid, glass, and cobalt-chromium-molybdenum alloys, later trademarked as Vitallium®, (7) over the next decades with fairly satisfactory results (Fig. 1). More and more materials were found to be biologically inert and useful for various types of procedures. Some were found by accident, like polymethylmethacrylate (PMMA). PMMA was found to be useful for ocular defects after examination of a WWII pilot who had small shards of his cockpit canopy, made of PMMA, embedded in his eye (8). Others were discovered by experimentation such as Vitallium® (7).

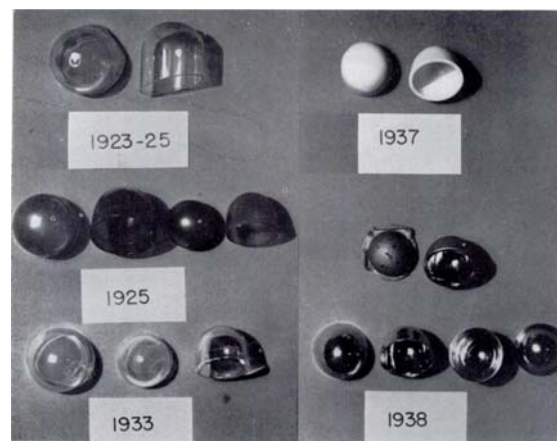


Fig. 1. Examples of materials used in early hip mold arthroplasty: 1923—glass, 1925—celluloid, 1933—glass, 1937—resin, 1938—Cobalt-chromium alloy (Reprinted with permission from (7))

Natural biomaterials were the next obvious material evolution in reparative materials because they contain similar architectures to the native tissue they are replacing along with many of the natural elements needed for proper tissue reconstruction. Human dermal grafts were researched very early on because of the necessarily similar structures and identical proteins to the humans in whom they were implanted. In 1936, Arthur Bowen wrote the first description of uses for porcine small intestinal submucosa. Development through animal models and *in vitro* testing lead to many implant applications for fixed and treated natural biomaterials. The first xenogenic sources for natural biomaterials were porcine and bovine in no small part because of their abundance. Recently attention has focused on bovine pericardium (9-12), bovine and porcine dermis (13-16), and porcine small intestinal submucosa (17-25), and cholecyst extracellular

matrix (26-28). The first patents for implants made from ECM biomaterials were issued in the 1970s for devices utilizing glutaraldehyde-fixed or freeze-dried biomaterials of porcine origin (29-31). By the 1980s, several methods of decellularizing xenographic material were developed and natural biomaterials became more widely to be used where synthetics were either unavailable or undesirable. Its ability to seemingly provoke a natural healing response and regenerate native host tissue rather than scar tissue (32) was of worth interest to. Many products that are currently on the market have been derived from a variety of bovine, porcine, and human tissues. Even limiting to a poll of two of the most successful ECM biomaterials, porcine SIS and human dermal tissue, the results show they have been used in over 1,000,000 patients (18,33).

Knowing the history of the development of biomaterials can give us a better perspective of how the state of the art is progressing. The big question with biomaterials is, “How will this product perform better than those available today?” It is all too easy, when performing research in today’s compartmentalized and specialized society to forget the bigger picture. The incremental changes made to modern natural biomaterials for a myriad of applications are made possible by continuous innovation by researchers, clinicians, and lay people. The market for ECM biomaterials is large and growing. The advanced wound care market alone was estimated at \$1.7 billion in 2003 (34) and the biomaterials market is projected to expand to \$3.7 billion by 2010 (35) Corporate and academic researchers alike recognize the value of using ECM biomaterials and are striving to create devices that use them in the most effective ways possible.

Research approaches

As shown, until the modern era, research approaches to biomaterials were spurred on by innovative and creative doctors who used whatever they thought might work to fix a problem sometimes with wonderful results but with extremely high risk. Today's researchers are much more focused into improving medicine methodically and with as little risk to patients as possible. While the road has been long and treacherous, nature has given us many amazing remedies put together by millions of years of evolution.

The complexity of ECM biomaterials defies simple explanation and this is one of their advantages. A typical biomaterial, manufactured using purified proteins may contain two or three parts such as collagen, elastin and maybe a polysaccharide. These parts are carefully measured, controlled, and uniform. ECM biomaterials are created *in vivo*, subject to a physiological

environment, stresses, and growth over the life of the donor (animal or human). All these signals, processes, and changes create a very intricate mixture of molecules and structural patterns. This mixture is one of the major advantages of ECM biomaterials. The body is able to incorporate the exact constituents necessary for tissue growth, maintenance, and repair into a tissue more effectively and efficiently than when attempted in a laboratory. Lucky for both manufacturers and patients, products may come to market without an exact specifications sheet, which could be supplied for any purely manufactured material. Products designed for ECM biomaterials must be designed around the known facts and observed results. Many of the questions that remain unanswered about ECM biomaterials do not adversely affect a product's ability to carry out its function or reside inside a patient. In fact, many of their properties enhance their product's performance.

Human dermal allografts are widely used as wound repair and scar prevention scaffolds (36-39), as dental prostheses (40,41), and in many reconstruction procedures (42-45). The benefits of using donated human dermis include abundance of the source, and similarity to the host tissue. Like all ECM biomaterials allografts contain many components that aide the natural healing and tissue regeneration process, reducing the amount of scarring and accelerating the rate of healing. Processing of dermal allografts includes decellularization and removal of all cellular remnants and so-called terminal sterilization. Terminal sterilization procedures such as ethylene oxide saturation or gamma irradiation attempt to package and seal the device so no contaminants can inadvertently be stored with the product.

Xenogenic prostheses are also widely used. Many of the benefits gained by using allografts are also attained using xenografts. Modern xenografts, mainly from porcine and bovine sources, comprise a large portion of the biomaterials market. One of the first bioprostheses was the artificial heart valve in the form of a glutaraldehyde-fixed porcine heart valve (31,46) or a glutaraldehyde-fixed bovine pericardium artificial valve (47). Glutaraldehyde-fixed prostheses are still used extensively, and efforts are continually being made to mitigate adverse long-term effects (48-52). These and other ECM biomaterials, prepared with and without glutaraldehyde are being used for a wide variety of procedures (Table 2).

Table 2. Applications of natural biomaterials.

Application	Natural Biomaterial
Artificial heart valves	Bovine pericardium Intact porcine aortic valves
Hernia repair devices	Porcine small intestinal submucosa Porcine urinary bladder mucosa Porcine dermal grafts
Sutures	Catgut (porcine or bovine intestinal wall)
Skin repair / wound care	Dermal allograft Porcine small intestinal submucosa Porcine dermal grafts
Vascular prostheses	Bovine ureter Porcine small intestinal submucosa Ovine arteries
Urethral repair	Porcine bladder
Breast reconstruction	Dermal allograft
Ligament repair	Dermal allograft Porcine small intestinal submucosa Fetal bovine skin
Spinal fusion / bone healing	Bone allografts

Development of ECM biomaterials can be divided into two major categories.

- **Physiological Reactions** – An ideal biomaterial should initiate the minimal immune response possible and allow cellular infiltration while maintaining its structure and performing its intended function. Eventually, it will then degrade and promote healthy tissue regeneration rather than fibrous scarring.
- **Mechanical Characteristics** – This category encompasses all the mechanical responses of the material to outside stimuli including the stress-strain response of the material to physiologically relevant loading, suture retention strength, and break strength.

A brief discussion of the modification of physiological responses to ECM biomaterials insofar as many of these modifications can affect the mechanical optimization is included, followed by a details of methods used to mechanically characterize and modify ECM biomaterials.

a. Physiological reactions

The physiological similarity of the biomaterial is probably the most important factor governing their ability to obtain approval for use. Native ECMs provoke a more natural healing response than synthetic materials (17), promoting cellular infiltration, proliferation, and differentiation into structures very similar to those of the uninjured host tissue. As previously discussed, many of the first ECM biomaterials were used in prostheses providing structural support or mechanical functionality (29-31). Consequently, preservation of the original structure and strength while reducing immunogenicity was paramount. The most abundant protein in ECMs is collagen, a fibrous protein which is remarkably preserved across species (53) and therefore invokes one of the weakest immune responses of all the proteins. This is, in fact, one reason natural collagen sutures implanted for thousands of years were so effective. The animal sinew composing the sutures is almost entirely collagen. Bovine collagen is still one of the most widely used and abundantly available xenogenic material used in biomedical applications (32).

Even though it is so well preserved, xenogenic collagen can still provoke immune reactions in humans who are hypersensitive to it or with extenuating circumstances (54-56). Typically, with proper cleaning with detergents and terminal sterilization by gamma irradiation or ethylene oxide gas is enough to reduce the immune response to a very minimal level, lower even than synthetic meshes (57-60). Immunogenic reactions to xenogenic collagen are caused by differences in telomeres, or repetitive end “buffer” sections, of the collagen molecules. These sections can be removed without harming the structural integrity of the protein molecule, however the processing breaks apart collagen fibers, greatly reducing the strength of any biomaterial made from that collagen. Atelomeric collagen does not form large fibrils like natural collagen therefore the strong networks found in ECM biomaterials cannot be replicated and telomeres cannot be effectively removed from ECM biomaterials. The benefits of improved healing response and biodegradability typically outweighs the small immune reaction from collagen.

Cells, their remnants and other biological matter in ECM biomaterials can cause immune reactions after implantation. Removal of these cellular components has been thoroughly researched and implemented to good effect. Accordingly, much of current research and development is concentrated on preparation treatments, enhancing desired properties such as strength, biodegradability, and reducing antigenicity. Crosslinking the material is a common way

to achieve these properties. A crosslinker physically or covalently bonds proteins together, modifying their properties as a result. Some can also act as sterilants, destroying cells within the matrix.

One of the most common crosslinkers in use today is glutaraldehyde. Glutaraldehyde kills cells quickly and creates permanent crosslinks between proteins. They are bound together due to the action of the dialdehydes on the ϵ -amino group of the lysyl residues in the protein. If a ECM biomaterial prosthetic is fully crosslinked by a strong glutaraldehyde solution, it becomes essentially non-biodegradable and will remain in the body until physically removed. Glutaraldehyde is also known to reduce the antigenicity of ECM biomaterials while making the prosthesis very resistant to infection (61). After implantation, over time, glutaraldehyde residues can leach into the host tissue and, due to its cytotoxic nature, cause the surrounding cells to die (62). The influx of calcium ions accompanying the presence of glutaraldehyde also contributes to calcification of the surrounding tissue(63) and can ultimately accelerate the failure of the implanted prosthesis (64).

The inherent disadvantages of glutaraldehyde fixation presented a large stumbling block for further material development, so other avenues were explored. Alternative chemical crosslinkers such as carbodiimides (21,65-67) and polyepoxy (68,69) provide similar mechanical strengthening and stiffening with reduced cytotoxic effects. The *in vivo* response to these chemically altered ECM biomaterials is much different than that of native ECMs (Fig. 2). Chemical fixatives reduce or eliminate the amount of cellular infiltration into the implant and can cause a foreign body reaction, typically forming a capsule around the device.

Physical crosslinking, comprising several steps of heating or compression, is advantageous because there are no chemical residues to cause concern for long term *in vivo* stability but the crosslinks are not always as effective as ones made with other methods. In contrast, dye-mediated photooxidation provides a more permanent effect. Several amino acids are capable of being oxidized by light while in the presence of specific photosynthesizing dyes (70,71). No chemical residues result from photooxidation and it has been shown that collagen matrices are stabilized to denaturation and enzymatic degradation. Crosslinking this way, uses the matrix's own structure leaving a more natural matrix after the process is completed (72). Physiologically, photooxidized biomaterials show very little host cell infiltration but low immunogenicity and high resistance to calcification (73,74).

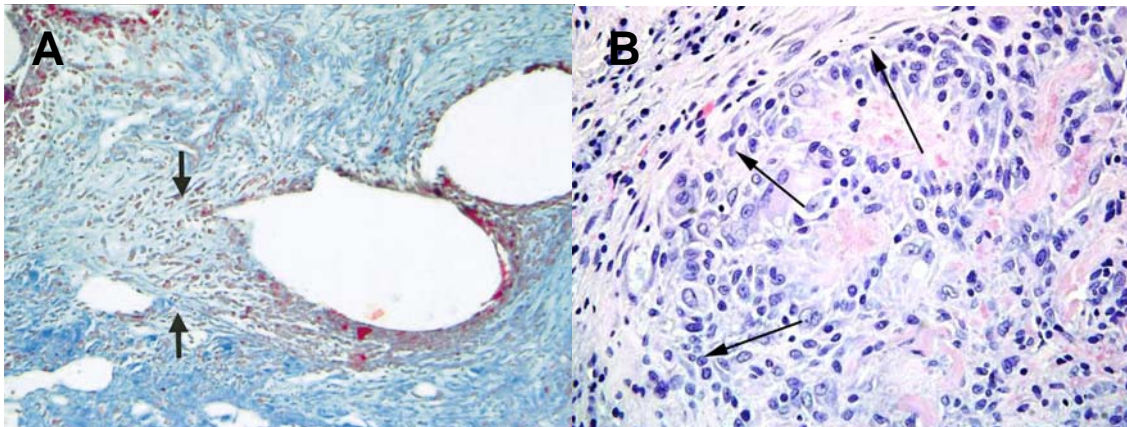


Fig. 2. a) Histologic appearance of the host tissue reaction to polyethylene mesh at 6 months post-surgery. The clear circular areas represent fibers of the polyethylene mesh. The surrounding spindle cells are embedded within a dense fibrous extracellular matrix and mononuclear cells (between arrows) at this 6-month time point. (Reproduced with permission from (17).) b) Histologic appearance of host tissue reaction to porcine-derived natural extracellular matrix (inside edge denoted by arrows). The implant has been heavily infiltrated with cells and is already being broken down at this three week time point.

Lastly, enzymatic crosslinkers provide a natural way to create crosslinks (75). In particular, transglutaminase (TGase) is an enzyme found in many organisms that catalyzes a reaction between glutamine residues the ϵ -amino groups of lysine residues (76). TGases crosslink in a more natural way than most other methods that can be applied by researchers because it is one of the crosslinkers used by the body. One disadvantage of most TGases is that its activity is dependent on the concentration of calcium ions present. One particular TGase derived from *Streptomyces mobaraensis*, referred to as microbial TGase (MTGase), is calcium independent giving it an advantage over other types (77). As a catalyst, MTGase leaves no residue and does not effect cell proliferation or attachment to the matrix (78). Research to improve the preparations of samples using MTGase show promise that it is a viable way to stabilize a collagen matrix against degradation (75,78,79).

Ultimately, a native ECM will be completely digested by the body's enzymatic processes within several weeks. Problems can occur when all the immunogenic material is not removed from a bioprosthetic device or cytotoxic and degradative factors negate the positive impacts of the device and lead to complications or even catastrophic failures (80). Rigorous testing maintains the high standard of current bioprostheses, while research strives to modulate to optimize ECM biomaterials to degrade at specific rates and maintain structural integrity for specific periods while still allowing cells to grow, infiltrate and heal in a natural way.

b. Mechanical characterization

Our primary stipulation about biomaterials was that they exist to repair, correct, or improve a physiological defect, deformation, or other malady through their implantation. A successfully designed device has to fit the mechanical requirements of the implant location. Tendon and soft tissue augmentation implants must be strong enough to withstand everyday forces applied to them by the patient. Prosthetic heart valves and vascular grafts must maintain their form under a constant flow of blood yet still be compliant enough to accommodate changes in pressure. Even wound dressings, which are not typically thought of as mechanical devices, must maintain their structure to allow infiltration of reparative cells, transport of nutrients, and transmission of biological signals. Just as the compositions ECM biomaterials are not simple, neither are their mechanical characteristics.

Collagen is found in all connective tissues in the body, in more than 27 identifiable types. Types I, II, III, V, and XI form fibrils and are found in tissues that must support mechanical stresses such as tendon, skin, cartilage, and bone (81). As these fibrous collagens are the major structural proteins in load bearing tissues, they significantly influence the mechanical characteristics of tissues. Large networks of small collagen fibrils afford many benefits over smaller networks of large fibrils. A review by Ottani *et al.* (82) describes the state of collagen fibrils in connective tissue. For any fibrous system, as long as the cross-sectional area of the fiber in a given section will be essentially unchanged, the tensile ultimate strength will be the same. Division of a fiber into multiple small fibrils affords two distinct benefits: the fiber has a great resistance to crack propagation and exhibits much better flexibility. Collagen molecules are very elastic and strong (tensile strength on the order of $1 \times 10^9 \text{N/m}^2$). Collagenous tissues typically fall into two categories. One composed of typically large, closely packed fibers of widely varying diameters. The other, composed of more uniform fibers of smaller average diameter and larger inter-fiber space (82). Variation in fiber diameter, length, and molecular packing work to exploit the strength of collagen to the utmost while allowing the overall properties of the tissue to change as required by the application.

Several tests are available to characterize natural biomaterials, any one of which can yield valuable information. Most natural biomaterials are hyperelastic and hyperelastic materials differ from linear elastic materials in that the initial relationship between stress and strain is initially linear but at some point the elastic modulus will increase based on a specific, typically

exponential, function (Fig. 3). This relationship is described by a strain energy density function which will be described later.

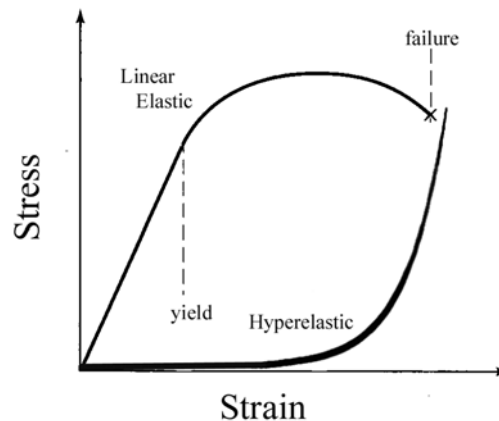


Fig. 3. Typical linear elastic and hyperelastic stress-strain curves. In the same strain that the linear elastic material experiences plastic yield and then failure, the hyperelastic material still deforms elastically.

1. Uniaxial and burst tests

The most common mechanical test is the uniaxial test tension test, which stretches a specimen through cycles or until fracture to observe the Young's modulus, or tensile modulus, and strength. Protocols for the uniaxial test vary but usually, a dogbone shaped specimen is placed in a pair of grips (Fig. 4a), which are separated by controlling the rate change in grip separation or specimen strain. Some anisotropic materials can be tested in several directions and the results aggregated to create a profile of the full material response (Fig. 4b). Uniaxial tensile and compression tests are most useful for elastic or pseudo-elastic solid materials such as plastics and metals used in orthopedic applications whose material properties vary linearly with strain and can be defined with only a few parameters. Softer, more compliant materials have minimal compressive strength, are difficult to grip, and are very difficult to test in this fashion. Consequently, researchers testing soft tissue adopted the easy to implement "ball burst test" specified to test textile strength by ASTM standard D3787-01.

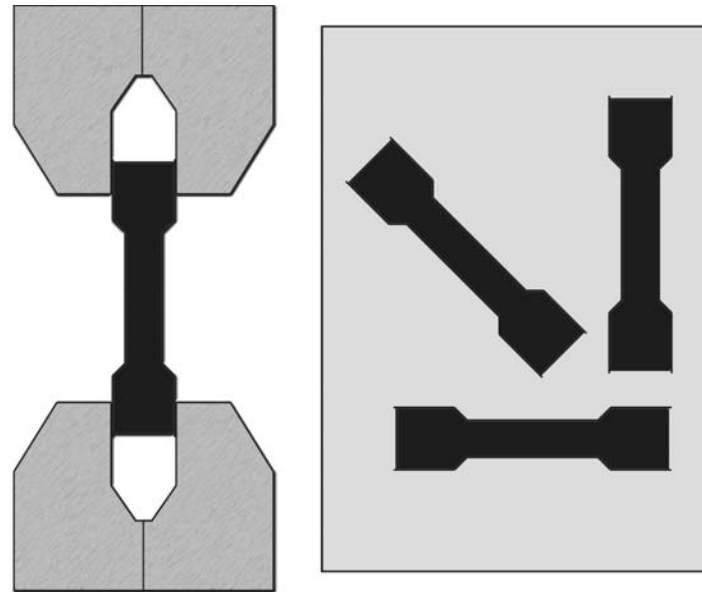


Fig. 4. a) Typical specimen shape, dubbed dog bone, mounted in the vice grips of a uniaxial testing platform b) Specimens can be cut in several directions from an anisotropic specimen

The burst test specifies that the thin sheet of material should be clamped in a ring, creating a taught sheet. Close attention must be paid in the case of natural biomaterials to make sure the slack is removed without actually stretching the tissue. In hyperelastic tissues, the initial 10-20% of stretch can occur with very little force. Once secured in the ring, a spherical plunger is pushed through the biomaterial at a slow rate until the sphere ruptures the biomaterial. The maximum force and distance the plunger moved at rupture can then be recorded. The exact dimensions of the apparatus, prescribed by the ASTM standard, allow a research group to compare materials they have tested but care must be taken when comparing results from different groups. Burst force and plunger travel distance are not intrinsic material quantities but can vary with the testing conditions.

To calculate intrinsic material properties, researchers can employ simple mathematical models. Freytes *et al.* (83) used a geometric mathematical model to predict the stresses and strains within the specimen while in the burst device (Fig. 5). With some calculation a Young's modulus equivalent called the maximum stress tensile modulus (MSTM) can be calculated. Because of their hyperelastic nature, natural biomaterials sustain much greater strains with a varying tensile modulus before they yield (Fig. 3). The MSTM simply measures the greatest slope on the

stress strain curve under the conditions of the test. Freytes *et al.* compared the results from their mathematical model with those from a finite element model for standard synthetic material. As expected, the finite element model was better able to delineate stress levels throughout the specimen, however the simple model accurately calculated the maximum stresses and strains. This implies that changes in these maximums from the mathematical model can be compared with any uniaxial test for a *rough* estimate of comparative strength. Because the standard ball burst test uses a single cycle to rupture, the biomaterial experiences no pre-conditioning and it has been shown that preconditioning dramatically changes the response of natural biomaterials (84) to loading. Pre-conditioning arguable replicates the state of a biomaterial when implanted. Biomaterials will rarely be subjected to a single dramatic mechanical stress upon implantation. Instead, *in situ*, biomaterials are subjected to the cyclic, periodic, and other varied loads occurring with every day movement.

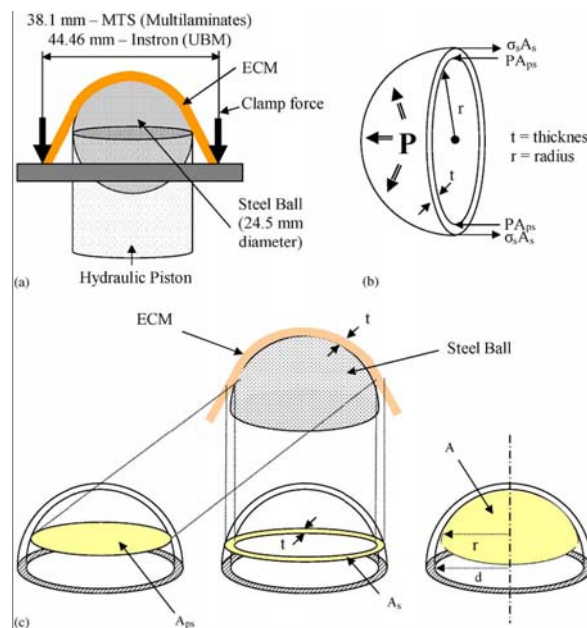


Fig. 5. (a) Dimensions of the ball-burst cage (b) Free body diagram of a thin wall spherical pressure vessel; (c) Definition of areas used in analysis (A_s ; A_{ps} , and A = different areas, t = initial thickness of the material, r = effect radius, ECM = extracellular matrix). (Reproduced with permission from (83)).

Recently, a new method for performing the burst test using an inflation device was developed by Billiar *et al.* (85) where the material was actually deformed in the ideal geometry of Freytes *et al.*'s mathematical model, making the calculations more accurate. This test

apparatus used water to inflate the biomaterial while measuring displacement with a laser extensometer and pressure, rather than the force, by means of a transducer in the burst chamber (Fig. 6). Cyclic, preconditioning tests can be performed as well because the water applies a uniform pressure to the entire surface of the biomaterial regardless of the state of inflation. Realistically, natural biomaterials are effectively cycled *in situ* as the body moves so this is an important step. A single cycle test records the initial loading reaction of a material with no unloading curve and no preconditioning. Natural biomaterials exhibit substantial changes between cycles but these can be reduced when the biomaterials are preconditioned under the same strains that will be implemented in subsequent tests (84) (Fig. 7).

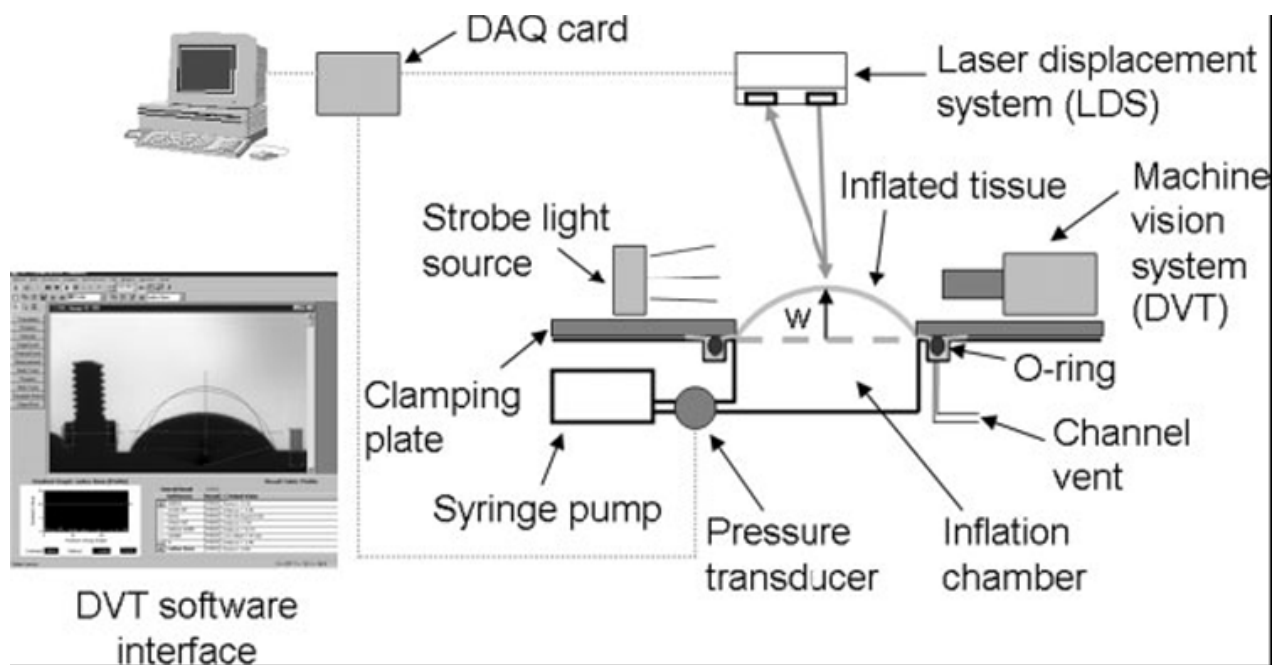


Fig. 6. Schematic of the membrane inflation system. A circularly clamped sample is inflated using a syringe pump as the pressure, central displacement (w), and radius of curvature are measured in real time and recorded. Inset: Digital video image of backlit sample used for image analysis. (Reproduced with permission from (85))

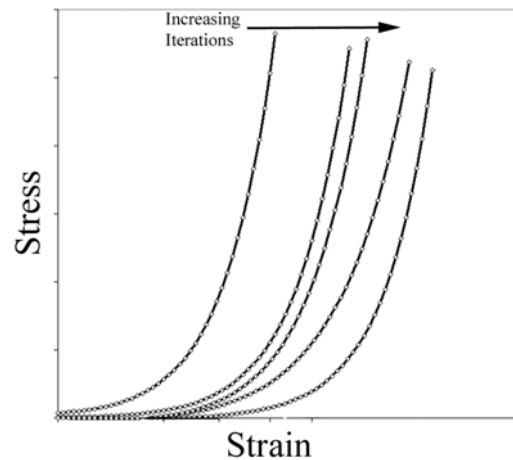


Fig. 7. Representation of the changes to the stress-strain profile of a natural biomaterial while being preconditioned. Once a stable stress-strain profile is reached, experimental data can be collected.

Burst tests are very useful for quick, easy, and accurate comparisons between multiple materials or treatment protocols under investigation. The water inflation device and mathematical model add a layer of complexity but greatly increase the usefulness of the data. The major limitation of both tests is that they impose conditions uniformity and isotropy, therefore any anisotropies, changes in thickness, or other variables are implicitly averaged out of the results.

2. Biaxial tests

The next level of mechanical testing is more complex but can assess anisotropic natural biomaterials and replicate stress states inside the body more accurately. Biaxial mechanical experiments control all four edges of a square specimen while allowing unconstrained changes in the thickness direction of the specimen. These tests were developed in 1948 by Treloar *et al.* (86) who first was able to apply two independent strains in orthogonal directions while measuring both strains independently.

One of the major obstacles to biaxial testing was to control each boundary while maintaining the degrees of freedom necessary to leave the other boundaries uninhibited. The techniques used to secure the specimens are especially important with very compliant, and sometimes fragile, materials such as natural biomaterials. The gripping mechanism must securely hold the specimen without doing damage or creating any unnecessary stress concentrations while

allowing the most independence of motion along the perpendicular axis, while equally distributing applied forces along the edge. Also because of its compliance, any strain measurements taken during such an experiment must be made sufficiently far away from the points where the specimens attach to the jig so as to avoid St. Venant's, strain concentration, effects (87).

There are many advantages to biaxial tests over more conventional, "simple", methods such as the uniaxial tension test or the burst test. A series of serial uniaxial tests with the tissue in different orientations cannot detect coupling that may be occurring within the tissue to modify the reaction to stress or strain in a particular direction. There is also evidence that a necking effect, similar to that dictated by Poisson's ratio in elastic tissues, can cause plastic deformation in the tissue. Burst tests incorporate coupling effects into a single test by stretching a material radially, though there is no way to separate these effects into their component parts and because the test is a single cycle to failure, the material never returns to an original unstressed state. Biaxial tests control two perpendicular axes independently and can pre-conditioning materials to a biologically relevant degree.

A few short years after Treloar developed his technique, Rivlin *et al.* (88) improved on it and were able to derive the constitutive equations for rubber by using only experimental observations. One of the most popular constitutive models for hyperelastic materials to this day is still the Mooney-Rivlin model. Research into the biaxial, planar properties of hyper-elastic materials improved in the ensuing years and was used extensively in new and emerging fields that required very precise models of complex loading problems such as aerodynamics. Because of the similarity in computational methods for both biomechanics and aerodynamics is not surprising then that biaxial testing was soon applied to natural biomaterials.

It was not until 1974 that the first attempt was made to use biaxial testing on biological tissues. Using an apparatus similar to Rivlin (88), Lanir and Fung (89,90) performed a detailed examination of the biomechanical properties of rabbit skin. Technological development has assuredly increased the precision and ease with which biaxial tests can be made but the principals are basically unchanged today.

A biaxial test machine is similar to two uniaxial testing machines laid on their side perpendicular to each other (Fig. 8). Each axis has a force gauge and independent actuators. Typically, a reservoir is fashioned to keep the tissue in simulated body fluid at body temperature

throughout the tests. A square of natural biomaterial is then attached to the actuators by several threads or sutures. Square specimens are used because other shapes have effects on the overall accuracy of results (91). Though it is more convenient to use a cross shaped specimen to maximize the unaffected “internal” area by keeping the points of attachment distant creates a non-uniform strain field, which invalidates many of the mathematical assumptions used to calculate the material properties. A square specimen provides the least distortion of the strain field and if the measurements are taken from the central 1/4(87) then effects from stress concentrations can be safely ignored.

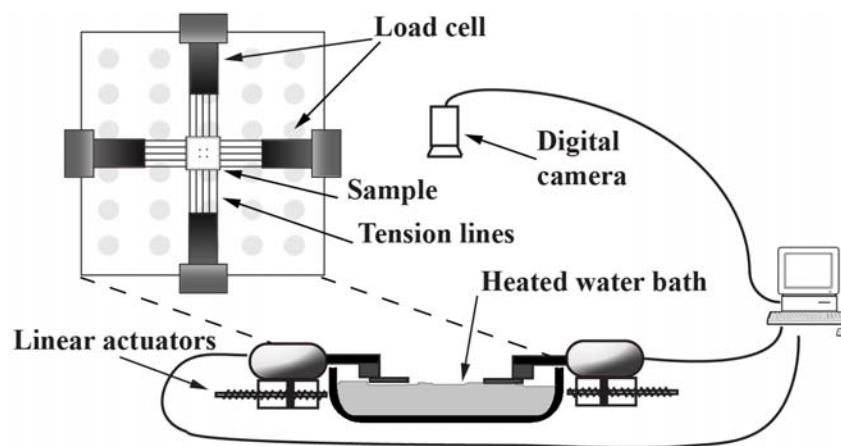


Fig. 8. Schematic of a biaxial testing system. A square specimen, marked with four dots for video strain measurement is immersed in a water bath and attached to four linear actuators using several thin lines. Floats can be placed on the attachment point of each line to maintain neutral buoyancy of the specimen. A computer controls the rate of strain using real-time feedback.

Each attachment suture must be independently adjustable to ensure that there are no unequal strains on the edges of the material. This can be accomplished with set screws, pulleys, or a combination of the two. This experimental design and setup allows this apparatus to apply strain along the orthogonal axes aligned with the square sides of the specimen with little or no shear. As each axis is tensioned and expands, the sutures move apart to accommodate the change in dimension, however the distance from point of attachment on the actuator to the specimen must be long enough that the forces are still essentially perpendicular (92).

Force is measured directly from load cells attached to the actuators and stress can be calculated. Deformation and subsequently strain is calculated by setting a camera above the specimen and tracking four or nine dots on the surface of the biomaterial away from the suture

attachments points. Newer, computer controlled machines calculate strain on the fly and are able to control the strain-rate precisely to give more accurate results. Because video systems are typically used to measure strain during biaxial tests, consideration must be given to the focal plane of the specimen. A natural biomaterial that is essentially neutrally buoyant in its natural state becomes much heavier when hooks, sutures, or other devices are attached to its edges. Keeping the specimen in the same vertical plane so that it neither goes out of focus nor changes size is paramount to accurate strain measurements. Some researchers have used floatation devices (87,93) as simple as small pieces of packing foam on each attachment point to counteract the added weight and keep the specimen at the surface of the bath. Others have used low friction glass platforms that support the biomaterial in the vertical direction while not impeding its expansion or contraction (Billiar *et al.* personal communication).

By varying the rate at which both sides are strained, different modes of strain, loading and cycling can be obtained. If the physiological range of stresses and strains is known, the material can be tested at those levels, otherwise it may be tested to find the envelope in which the material will not fail or plastically deform. Results from these types of biaxial tests are very useful when determining the usability of a natural biomaterial in a specific application, the relative strength advantages over other natural biomaterials or, of course, for characterizing the mechanical properties of a natural biomaterial.

3. Identifying fiber orientation

Interspecimen variability can be very high when using natural biomaterials and can result in poor agreement between results of different specimen sets or research groups. Natural biomaterial specimens are generally not isotropic because of the many random fibers that compose the framework of natural tissues. Even within specimens taken from a single subject, results of mechanical tests can differ greatly depending on a variety of factors. One way of reducing this variability is to identify the principal axes of the material. The principal axis is the direction in which the greatest numbers of material fibers are oriented. Because of the large number of fibers, the principal axis of a material is the “strongest” axis. Consequently, the axis perpendicular to the principal axis is the weakest. Biaxially testing along these axes will give a maximum and minimum stress-strain profile of the material. Because of the way natural biomaterials grow, more fibers tend to align to the directions of greatest load. If a researcher can directly measure

these fibers, anatomic variations no longer play a role in specimen testing and the errors caused by them are reduced.

While determining the principal axes and degree of anisotropy is relatively simple with synthetic materials, which are made to exact specifications, there are no blueprints for natural biomaterials. Each parameter must be observed directly or experimentally derived. In some cases such as muscle and tendon, microscopic inspection can reveal the dominant fiber direction. In many cases however, the fibers are quite small and challenging to discern. Several methods have been developed to determine the orientations of these fibers.

Fiber orientations in natural biomaterials have been studied with techniques such as electron microscopy (94) and standard polarized light microscopy (95). These techniques, while effective in a limited scope, can only acquire local information and are very time consuming. A real time method would give a researcher a good understanding of the basic reactions a natural biomaterial will have *in situ*.

In 1990, a report by Choi and Vito (96) presented a study in which the biaxial properties of canine pericardium using an improved biaxial testing apparatus that allowed real-time feedback control of the strain rate and the ability to calculate both normal and shear strains. Problems of interspecimen variability (97) led Choi and Vito to develop a possible solution to this problem. The researchers took a circular piece of each specimen and attached suture loops to it at 15° increments. One pair of sutures was then mounted to a testing device that applied only enough tension to take the slack out of the tissue and then held the length between those sutures constant. Approximately 1N of force was then applied along the orthogonal diameter. The force stretched the tissue along that orthogonal direction and two marks were made along the stretched diameter with enamel ink 5.0cm apart. The specimen was then rotated 15° and the procedure repeated for 180°. When all possible pairs were marked, the tissue was released and allowed to relax to its unstressed state. The dots made at 5cm apart under tension created an ellipse in the relaxed state whose major and minor axes coincided with the with material symmetry axis, the minor axis representing the axis of maximum stiffness and the major axis necessarily representing the axis of maximum compliance. The ratio of the major axis to the minor axis was also an accurate representation of the anisotropy of the specimen compared to the material constants calculated after complete testing of the material. These axes were measured with respect to a predefined anatomical axis and it was found that this angle varied widely between

specimens, possibly contributing to the previously reported interspecimen variability and inconsistent assessments of material symmetry (98,99).

Choi and Vito's study also raised the issue of improper or inaccurate measurement of sample size. Changes made in preconditioning are not permanent and may sometimes actually change between trials of the same specimen. As we stated earlier, a hyperelastic material is defined by the change in the deformation gradient and is depending on both the initial state and "current" state. Only when the initial state is defined accurately can a material's properties be accurately measured.

Indirect methods can also be used to determine the principal material axes of natural biomaterials. Small Angle Light Scattering (SALS) was adapted by Kronick and Sacks (100) to identify the orientations of collagen fibers in cattle hide. The technique had already been used to determine the quantity of collagen and elastin in tissues and the fiber orientation results were verified against x-ray diffraction results (101). In the SALS technique, laser light is passed through a tissue and uses the intensity of the resulting scattered light to reconstruct an average underlying structure. Using laser light of a wavelength on the same order of size as collagen and elastin fibers ensures the light will be refracted by those specific molecules. The network of fibers acts like a group of single slits. Measuring the intensity of light at 1° increments around the central optical axis provided an intensity distribution that coincided with the natural biomaterial's primary fiber angles (100). The principle of SALS is very similar to that used by Vito *et al.* except this method required no physical intervention. It can also be done concurrently to a biaxial test without altering the specimen, giving a snapshot view of the specimen before and after strain is applied. Whereas the mechanical method of determining the principal mechanical axis of the material finds a bulk axis that was an average of the whole surface, SALS determines the fiber orientations at discrete points in the material. The discrete orientations can be coalesced to form a map of the fiber orientations over the surface of the material which is very accurate.

Similarly to SALS, Polarized light microscopy (PLM) and birefringence can be used to qualitatively determine fiber directions (95,102). Birefringence, or double refraction, is when a ray of light passing through a material decomposes into two rays depending on polarization of the light (103). When the light is split, the resulting rays have different velocities and when they are recombined in the analyzer of the microscope, they create constructive and destructive interference patterns (Fig. 9). The interference patterns (Fig. 10) are measured and the angle of

the predominant internal structure of the material can be calculated from the sine of the phase difference,

$$\delta = 2\pi L(n_2 - n_1) / \lambda$$

where L is the sample thickness, n_x are the refractive indices of the material, λ is the wavelength of the light, and δ is the phase difference of the light (104). Unfortunately, this equation is ambiguously defined when only using image intensities and exact measurements cannot be derived. A quantitative method was developed using the rotating polarizer method and additional algorithms to remove the ambiguity. Geday *et al.* provide a detailed discussion of this method and its derivation (104). Typically, assessment of the fiber orientations of a specimen is performed before and/or after a mechanical test, showing an instant of the material's state.

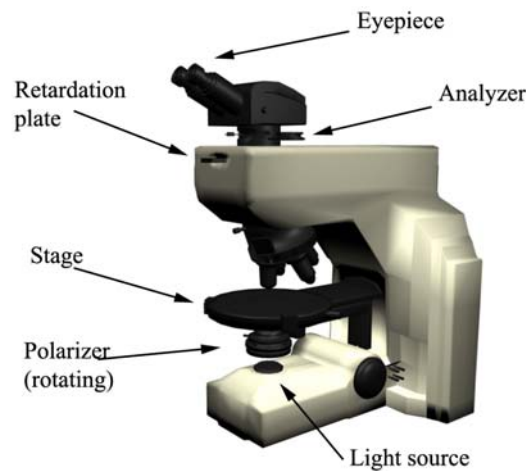


Fig. 9. Diagram of a polarized light microscope showing the location of the specialized components. A birefringent material on the stage transmits a characteristic interference pattern at each angle of polarized light. The rotating polarizer facilitates analysis of multiple angles for a complete picture of a biomaterial.

A new polarized light method, developed by Tower *et al.* as an upgrade to previous PLM techniques, assesses the fiber alignment of natural biomaterials in real time. The specimen is mounted in the microscope and loaded by a mechanical testing apparatus while the fiber orientations are detected over large areas of the tissue, enabling tracking of fiber orientations throughout mechanical tests (105). The analyzer accomplishes this by detecting the sinusoidal oscillations in the light intensity passing through the birefringent material, in this case a natural biomaterial. These oscillations are directly related to the orientation of the fibers in the material, which can then be determined for each pixel in the image. This method is advantageous over

standard PLM in that it provides quantitative real time data rather than qualitative measurements (105).

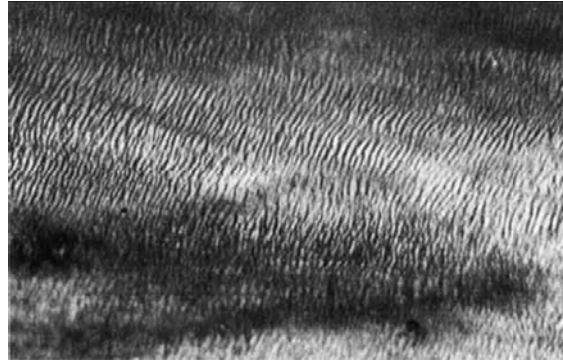


Fig. 10. A low-magnification polarized light microscopy image of a midcusp region of a porcine aortic valve leaflet showing a characteristic banding pattern representing crimped collagen bundles. (Reproduced with permission)

4. Material modeling

Finally, with all this available data for a material, we are able to apply a model that will predict how the material will react when different stresses are applied. Modeling allows experimentation to happen inside a computer where there are unlimited supplies of materials and fabrication is just a few clicks away. Designs can be tested in a finite element modeling program, yielding results that are far more precise than any real world experiment could be.

Before delving into what material models are and how they are used, we have to define a few terms mathematically for clarity. The change in position of a given point during a biaxial test can be described by the following:

$$x_1 = \lambda_1 X_1 + \kappa_1 X_2 \qquad x_2 = \lambda_2 X_1 + \kappa_2 X_2 \qquad x_3 = \lambda_3 X_3$$

Where X and x are the position coordinates in the undeformed and deformed states, respectively. The λ variables are the stretch ratios along each axis and κ are measures of shear in the plane of the material. The nature of the biaxial test prohibits there being any shear in the x_3 direction. Using this information, the entire deformation state of a material can be described by the deformation gradient, \mathbf{F} . The deformation gradient describes the changes in deformed position over all the original points and can be displayed in differential and matrix notation as follows:

$$\mathbf{F} = \frac{\partial \mathbf{x}}{\partial \mathbf{X}} = \begin{bmatrix} \lambda_1 & \kappa_1 & 0 \\ \kappa_2 & \lambda_2 & 0 \\ 0 & 0 & \lambda_3 \end{bmatrix}$$

\mathbf{F} is asymmetric but because natural biomaterials can be thought of as incompressible tissues due to their very high water content, it is mathematically constrained in its values to preserve the volume of the biomaterial.

The next logical step in describing the material response is utilizes strain, which is a non-dimensional way to describe physical expansion or contraction with respect to a reference position. In this case, we are using Green-Lagrange strain \mathbf{E} to describe the deformation with respect to the original unloaded state. This can be calculated directly from \mathbf{F} :

$$\mathbf{E} = \frac{1}{2}(\mathbf{F}^T \mathbf{F} - \mathbf{I})$$

Where \mathbf{I} is the identity matrix and \mathbf{E} is a symmetric matrix. Practically, this is one of the easiest forms of strain to compute and consequently, is one of the most popular formulations.

Finally, the most common measure of stress, the second Piola-Kirchoff stress, \mathbf{S} , is calculated using force/unit area and stretch ratio measurements. The 2nd P-K stress, like Green's strain, is a symmetric quantity. These symmetries come in handy when formulating models. Here again, the design of the biaxial test simplifies the calculations necessary to find the stress. Because the natural biomaterial is basically a thin film, the stress in the thickness-direction (3) is assumed to be zero. Additionally, because the apparatus applies stress perpendicular to the sides of the square specimen, it induces negligible shear. As a result, only two stress components need to be calculated:

$$\mathbf{S}_{11} = \left(\frac{P_1}{hL_2} \right) \frac{1}{\lambda_1} \quad \mathbf{S}_{22} = \left(\frac{P_2}{hL_1} \right) \frac{1}{\lambda_2}$$

Where P is the force (because we already used \mathbf{F} for the deformation gradient, h is the specimen height or thickness, and L is the specimen side length perpendicular to the force.

An elastic material's behavior can be determined independently anywhere at any moment according to \mathbf{F} . A hyperelastic material responds to stress and strain according to the rate of change in the deformation gradient $\dot{\mathbf{F}}$ meaning that it is dependent on both the initial state at time $t = 0$ and the final state at time t but it is independent from the path used to get from time 0 to t . (106). This leads us to the development of a strain energy function $W(\mathbf{F})$, mentioned earlier,

which is a function of the deformation gradient, that completely describes the internal energy of the material due to the external forces acting upon it. Because it is a function of \mathbf{F} , W can also be described as a function of \mathbf{E} . Generally, the strain energy equation is very difficult to solve, but by designing experiments correctly, researchers reduced the number of necessary parameters. Because natural biomaterials are incompressible, one degree of freedom is removed from the system. Properly designed biaxial tests produce negligible shear in test specimens, further reducing the complexity (92). Many different strain energy functions can be used to describe a material. Choosing the most effective and least computationally costly method is a large part of deciphering the correct properties for a material.

Luckily, researchers have already come up with ways of reducing the parameters of the strain energy equation and have developed models that fit most of the materials (natural, synthetic, or otherwise). Using their models, we can produce material constants that describe the material responses to other stresses and strains without the need for exhaustive experimental testing. The accuracy of the simulations depends on the accuracy of the experimental data used to make the model. With a little planning this accuracy can be very high.

Since the first experiments on rabbit skin, modeling has been one of the goals of biaxial testing and mechanical characterization. The strain-energy equation, is the key to material modeling. Tong and Fung (107) used the data they gathered on rabbit skin to build an equation that they thought might describe their specimens. Firstly, despite observed hysteresis in the loading and unloading curves, the load responses were basically strain-rate independent. Additionally, the principal axis of anisotropy or principal material axis varied based on the specimen's anatomic orientation. Lastly, the specimens exhibited a biphasic behavior, initially very compliant then stiffening very rapidly. Due to the strain-rate insensitivity of the natural biomaterials, Tong and Fung were able to develop separate strain-energy functions for the loading and unloading states, thereby simplifying the problem. After fitting the data to several iterations of a basic strain energy functions, the most effective equation was decided upon:

$$\rho_0 W = \frac{c}{2} \left(\exp \left[a_1 E_{11}^2 + a_2 E_{22}^2 + a_4 E_{11} E_{22} \right] - 1 \right)$$

Where ρ_0 is the initial density of the material, c is a constant multiplier, and a_i are material constants. The constant a_3 has been omitted because it accompanied the shear term of this equation. The general form of this equation had 15 terms, most of which were eliminated

because of the negligible effect they had on the accuracy of the model. This model, called the “Fung” model, is a good approximation of many natural biomaterials and is used widely in the field.

The more data added to the model, the better the results are. Due to the difficulty of controlling the stress applied to each side accurately in real time, most protocols call for strain controlled trials. An effective set of data for a model must have both equibiaxial strain trials and several different non-equibiaxial strain ratio trials. Trials using strain ratios equally spaced around both axes, such as a regime of $\varepsilon_1 : \varepsilon_2 = 8:1, 4:1, 2:1, 1:1, 1:2, 1:4, 1:8$ provide a good starting point. Increasing the number of trials and strain ratios will provide a larger base from which the model can extrapolate the overall material properties. Too few trials will cause the model to make good predictions for that particular loading regime very well but makes it more likely to make poor predictions for any other loading regime it may encounter. Particularly, do not try to create a fit with data gathered from only a single strain ratio set of experiments, the strain energy density equation is particularly weak. In the Fung model, the constant relationship between E_{11} and E_{22} produces mathematical collinearities and can result in an inaccurate model. It is important to remember to ensure the conditions you are obtaining in your experiments are relevant to the application for which you are testing. Creating a complete material model for a natural biomaterial that is valid under all conditions is a much more daunting task than creating a model that is optimized for a precise range. For example, when designing an implant for an abdominal wall patch, pressures of 16MPa are not expected and pressures of 0.1kPa are going to be dominated by larger factors.

Many mathematical models have been developed subsequent to the Fung model (97,108,109) each improving on certain aspects of the previous formulations and arriving at a constitutive model that more accurately describes the data gathered in a certain set of experiments. The decision of which model to use is an important step in any biomaterials research. Appropriate models for natural biomaterials can be found in the literature and within any of several finite element modeling packages that are commercially available. Finite element packages simplify the task of generating models immensely by only requiring the biaxial data to be entered by the user, generating all the coefficients automatically once the desired model is chosen. The more data they are given, the more accurate the model. Using the experimental guidelines provided here, these models can be invaluable to experimentalists with expensive or

hard to process materials. After the model is verified, virtual design changes can be made, virtual loading conditions altered until a real “final draft” is ready to be produced and tested.

Conclusions

Any biomaterial implanted into the body has to interface well with the existing tissue while performing its function. The obvious implication of that statement is that the body receiving the implant should not reject it physiologically. The more subtle, but equally significant implication is that the mechanical properties of the implant should be appropriate for the location in which it is implanted. This entails insuring the correct anisotropy is maintained and the material responds appropriately to mechanical stimuli. Sometimes empirical evidence through simple burst or biaxial tests is all that is needed for confirmation. Other times, it is necessary and convenient to find the natural biomaterial's properties and model using finite element analysis, expanding the limits of what experiments and conditions can be tested. Just as a structural engineer is able to determine if a high rise building will withstand the forces of strong winds when it is full erected before construction ever begins, a biomedical engineer can use these data to determine if an implant will fail mechanically when subjected to the wear and tear of daily living inside a person. We have come a long way from the beginnings of natural biomaterial implantation and we are at a point when the available technology intersects with the desire for knowledge. All of today's available tools can yield valuable and accurate information. It only depends on the researcher to choose how much information they need and how best to use it.

Acknowledgements.

I would like to acknowledge Krishna Burugapalli and Michelle Menard for their help with figures in this chapter.

References

1. Ratner BD. 2006. Biomaterials Tutorial: An Introduction to Biomaterials. University of Washington Engineered Biomaterials <<http://www.uweb.engr.washington.edu/research/tutorials/introbiomat.html>>. Accessed on 5th June 2007
2. Ratner BD, Hoffman AS, Schoen FJ, Lemons JE. Biomaterials Science: An Introduction to Materials in Medicine. New York: Academic Press; 1996. p 1-10,84-94.
3. Zimmerman LM, Veith I. Great Ideas in the History of Surgery. New York: Norman Publishers; 1993. 587 p.
4. Maluf NS. History of blood transfusion. J Hist Med Allied Sci 1954;9(1):59-107.
5. Sanan A, Haines SJ. Repairing holes in the head: a history of cranioplasty. Neurosurgery 1997;40(3):588-603.
6. Slavkin HC. Biomimicry, dental implants and clinical trials. J Am Dent Assoc 1998;129(2):226-30.
7. Smith-Petersen MN. Evolution of Mould Arthroplasty of the Hip Joint. J Bone Joint Surg 1948;30B(1):59-75.
8. Ratner BD, Bryant SJ. Biomaterials: where we have been and where we are going. Annu Rev Biomed Eng 2004;6:41-75.
9. Al Halees Z, Al Shahid M, Al Sane'i A, Sallehuddin A, Duran C. Up to 16 years follow-up of aortic valve reconstruction with pericardium: a stentless readily available cheap valve? Eur J Cardiothorac Surg 2005;28(2):200-5; discussion 205.
10. Chang Y, Chen SC, Wei HJ, Wu TJ, Liang HC, Lai PH, Yang HH, Sung HW. Tissue regeneration observed in a porous acellular bovine pericardium used to repair a myocardial defect in the right ventricle of a rat model. J Thorac Cardiovasc Surg 2005;130(3):705-11.
11. Neethling WM, Hodge AJ, Clode P, Glancy R. A multi-step approach in anti-calcification of glutaraldehyde-preserved bovine pericardium. J Cardiovasc Surg (Torino) 2006;47(6):711-8.
12. Wei HJ, Chen SC, Chang Y, Hwang SM, Lin WW, Lai PH, Chiang HK, Hsu LF, Yang HH, Sung HW. Porous acellular bovine pericardium seeded with mesenchymal stem cells as a patch to repair a myocardial defect in a syngeneic rat model. Biomaterials 2006;27(31):5409-19.
13. Derwin KA, Baker AR, Spragg RK, Leigh DR, Iannotti JP. Commercial extracellular matrix scaffolds for rotator cuff tendon repair. Biomechanical, biochemical, and cellular properties. J Bone Joint Surg Am 2006;88(12):2665-72.
14. Gandhi S, Kubba LM, Abramov Y, Botros SM, Goldberg RP, Victor TA, Sand PK. Histopathologic changes of porcine dermis xenografts for transvaginal suburethral slings. Am J Obstet Gynecol 2005;192(5):1643-8.
15. Kelley P, Gordley K, Higuera S, Hicks J, Hollier LH. Assessing the long-term retention and permanency of acellular cross-linked porcine dermal collagen as a soft-tissue substitute. Plast Reconstr Surg 2005;116(6):1780-4.
16. Kimuli M, Eardley I, Southgate J. In vitro assessment of decellularized porcine dermis as a matrix for urinary tract reconstruction. BJU Int 2004;94(6):859-66.
17. Badylak S, Kokini K, Tullius B, Simmons-Byrd A, Morff R. Morphologic study of small intestinal submucosa as a body wall repair device. J Surg Res 2002;103(2):190-202.
18. Badylak SF. Xenogeneic extracellular matrix as a scaffold for tissue reconstruction. Transpl Immunol 2004;12(3-4):367-77.
19. Badylak SF, Lantz GC, Coffey A, Geddes LA. Small intestinal submucosa as a large diameter vascular graft in the dog. J Surg Res 1989;47(1):74-80.
20. Brown-Etris M, Cutshall WD, Miles MC. A New Biomaterial Derived From Small Intestine Submucosa and Developed Into a Wound Matrix Device. Wounds 2002;14(4):150-166.

21. Kim MS, Hong KD, Shin HW, Kim SH, Kim SH, Lee MS, Jang WY, Khang G, Lee HB. Preparation of porcine small intestinal submucosa sponge and their application as a wound dressing in full-thickness skin defect of rat. *Int J Biol Macromol* 2005;36(1-2):54-60.
22. Zhang Y, Frimberger D, Cheng EY, Lin HK, Kropp BP. Challenges in a larger bladder replacement with cell-seeded and unseeded small intestinal submucosa grafts in a subtotal cystectomy model. *BJU Int* 2006;98(5):1100-5.
23. Hauser S, Bastian PJ, Fechner G, Muller SC. Small intestine submucosa in urethral stricture repair in a consecutive series. *Urology* 2006;68(2):263-6.
24. John T, Bandi G, Santucci R. Porcine small intestinal submucosa is not an ideal graft material for Peyronie's disease surgery. *J Urol* 2006;176(3):1025-8; discussion 1029.
25. Iannotti JP, Codsí MJ, Kwon YW, Derwin K, Ciccone J, Brems JJ. Porcine small intestine submucosa augmentation of surgical repair of chronic two-tendon rotator cuff tears. A randomized, controlled trial. *J Bone Joint Surg Am* 2006;88(6):1238-44.
26. Brody S, McMahon J, Yao L, O'Brien M, Dockery P, Pandit A. The effect of cholecyst-derived extracellular matrix on the phenotypic behaviour of valvular endothelial and valvular interstitial cells. *Biomaterials* 2007;28(8):1461-9.
27. Burugapalli K, Thapasimuttu A, Chan JC, Yao L, Brody S, Kelly JL, Pandit A. Scaffold with a natural mesh-like architecture: isolation, structural, and in vitro characterization. *Biomacromolecules* 2007;8(3):928-36.
28. Coburn JC, Brody S, Billiar KL, Pandit A. Biaxial mechanical evaluation of cholecyst-derived extracellular matrix: a weakly anisotropic potential tissue engineered biomaterial. *J Biomed Mater Res A* 2007;81(1):250-6.
29. Angell WWY, D.L.; Angell, W.W., assignee. Heart Valve Stent. USA patent 3983581. 1976.
30. Dewanjee MR; Mayo Foundation, assignee. Treatment of Collagenous Tissue with Glutaraldehyde and Aminodiphosphoate Calcification Inhibitor. USA patent 4553974. 1985.
31. Liotta DS, Ferrari HM, Pisanu AJ, Donato FO; Low Profile Glutaraldehyde-fixed Porcine Aortic Prosthetic Device. USA patent 4079468. 1978.
32. Badylak SF. The extracellular matrix as a scaffold for tissue reconstruction. *Semin Cell Dev Biol* 2002;13(5):377-83.
33. 2006. LifeCell's Technology. <www.lifecell.com/corporate/15/>. Accessed on 20th June 2007
34. Elder MA. Markets for Advanced Wound Care Tehnologies. Business Communication Company Inc.; 2004 December 2004. Report nr PHM011D.
35. Biocompatible Materials. Freedomia Group Inc.; 2006.
36. Cuono C, Langdon R, McGuire J. Use of cultured epidermal autografts and dermal allografts as skin replacement after burn injury. *Lancet* 1986;1(8490):1123-4.
37. Bello YM, Falabella AF, Eaglstein WH. Tissue-engineered skin. Current status in wound healing. *Am J Clin Dermatol* 2001;2(5):305-13.
38. Lu V, Johnson MA. Tracheostomy scar revision using acellular dermal matrix allograft. *Plast Reconstr Surg* 2004;113(7):2217-9.
39. Wainwright D, Madden M, Luterman A, Hunt J, Monafó W, Heimbach D, Kagan R, Sittig K, Dimick A, Herndon D. Clinical evaluation of an acellular allograft dermal matrix in full-thickness burns. *J Burn Care Rehabil* 1996;17(2):124-36.
40. Peacock ME, Cuenin MF, Hokett SD. Gingival augmentation with a dermal allograft. *Gen Dent* 1999;47(5):526-8.
41. Wei PC, Laurell L, Lingen MW, Geivelis M. Acellular dermal matrix allografts to achieve increased attached gingiva. Part 2. A histological comparative study. *J Periodontol* 2002;73(3):257-65.
42. Miklos JR, Kohli N, Moore R. Levatorplasty release and reconstruction of rectovaginal septum using allogenic dermal graft. *Int Urogynecol J Pelvic Floor Dysfunct* 2002;13(1):44-6.
43. Lorenz RR, Dean RL, Hurley DB, Chuang J, Citardi MJ. Endoscopic reconstruction of anterior and middle cranial fossa defects using acellular dermal allograft. *Laryngoscope* 2003;113(3):496-501.

44. Griffin TJ, Cheung WS, Hirayama H. Hard and soft tissue augmentation in implant therapy using acellular dermal matrix. *Int J Periodontics Restorative Dent* 2004;24(4):352-61.
45. Kolker AR, Brown DJ, Redstone JS, Scarpinato VM, Wallack MK. Multilayer reconstruction of abdominal wall defects with acellular dermal allograft (AlloDerm) and component separation. *Ann Plast Surg* 2005;55(1):36-41; discussion 41-2.
46. Carpentier A, Deloche A, Relland J, Fabiani JN, Forman J, Camilleri JP, Soyer R, Dubost C. Six-year follow-up of glutaraldehyde-preserved heterografts. With particular reference to the treatment of congenital valve malformations. *J Thorac Cardiovasc Surg* 1974;68(5):771-82.
47. Ross DN. Flexible bioprosthetic pericardial heart valve. *Thorac Cardiovasc Surg* 1980;28(2):150-2.
48. Corno AF, Hurni M, Griffin H, Jeanrenaud X, von Segesser LK. Glutaraldehyde-fixed bovine jugular vein as a substitute for the pulmonary valve in the Ross operation. *J Thorac Cardiovasc Surg* 2001;122(3):493-4.
49. Lee WK, Park KD, Kim YH, Suh H, Park JC, Lee JE, Sun K, Baek MJ, Kim HM, Kim SH. Improved calcification resistance and biocompatibility of tissue patch grafted with sulfonated PEO or heparin after glutaraldehyde fixation. *J Biomed Mater Res* 2001;58(1):27-35.
50. Meuris B, Phillips R, Moore MA, Flameng W. Porcine stentless bioprostheses: prevention of aortic wall calcification by dye-mediated photo-oxidation. *Artif Organs* 2003;27(6):537-43.
51. Neethling WM, Cooper S, Van Den Heever JJ, Hough J, Hodge AJ. Evaluation of kangaroo pericardium as an alternative substitute for reconstructive cardiac surgery. *J Cardiovasc Surg (Torino)* 2002;43(3):301-6.
52. Sucu N, Karaca K, Yilmaz N, Comelekoglu U, Aytacoglu BN, Tamer L, Ozeren M, Dondas HA, Oguz Y, Ogenler O and others. Two stage EDTA anti-calcification method for bioprosthetic heart valve materials. *Med Sci Monit* 2006;12(6):MT33-8.
53. van der Rest M, Garrone R. Collagen family of proteins. *Faseb J* 1991;5(13):2814-23.
54. Klein B, Schiffer R, Hafemann B, Klosterhalfen B, Zwadlo-Klarwasser G. Inflammatory response to a porcine membrane composed of fibrous collagen and elastin as dermal substitute. *J Mater Sci Mater Med* 2001;12(5):419-24.
55. Zheng MH, Chen J, Kirilak Y, Willers C, Xu J, Wood D. Porcine small intestine submucosa (SIS) is not an acellular collagenous matrix and contains porcine DNA: possible implications in human implantation. *J Biomed Mater Res B Appl Biomater* 2005;73(1):61-7.
56. Dzemeshkevich SL, Konstantinov BA, Gromova GV, Lyudinovskova RA, Kudrina LL. The mitral valve replacement by the new-type bioprostheses (features of design and long-term results). *J Cardiovasc Surg (Torino)* 1994;35(6 Suppl 1):189-91.
57. Allman AJ, McPherson TB, Badylak SF, Merrill LC, Kallakury B, Sheehan C, Raeder RH, Metzger DW. Xenogeneic extracellular matrix grafts elicit a TH2-restricted immune response. *Transplantation* 2001;71(11):1631-40.
58. Patino MG, Neiders ME, Andreana S, Noble B, Cohen RE. Cellular inflammatory response to porcine collagen membranes. *J Periodontol Res* 2003;38(5):458-64.
59. Konstantinovic ML, Lagae P, Zheng F, Verbeken EK, De Ridder D, Deprest JA. Comparison of host response to polypropylene and non-cross-linked porcine small intestine serosal-derived collagen implants in a rat model. *Bjog* 2005;112(11):1554-60.
60. O'Neill P, Booth AE. Use of porcine dermis as a dural substitute in 72 patients. *J Neurosurg* 1984;61(2):351-4.
61. Schechter I. Prolonged retention of glutaraldehyde-treated skin allografts and xenografts: immunological and histological studies. *Ann Surg* 1975;182(6):699-704.
62. Huang-Lee LL, Cheung DT, Nimni ME. Biochemical changes and cytotoxicity associated with the degradation of polymeric glutaraldehyde derived crosslinks. *J Biomed Mater Res* 1990;24(9):1185-201.
63. Kim KM, Herrera GA, Battarbee HD. Role of glutaraldehyde in calcification of porcine aortic valve fibroblasts. *Am J Pathol* 1999;154(3):843-52.

64. Schoen FJ, Levy RJ. Calcification of tissue heart valve substitutes: progress toward understanding and prevention. *Ann Thorac Surg* 2005;79(3):1072-80.
65. Girardot JM, Girardot MN. Amide cross-linking: an alternative to glutaraldehyde fixation. *J Heart Valve Dis* 1996;5(5):518-25.
66. Weadock K, Olson RM, Silver FH. Evaluation of collagen crosslinking techniques. *Biomater Med Devices Artif Organs* 1983;11(4):293-318.
67. Buttafoco L, Engbers-Buijtenhuijs P, Poot AA, Dijkstra PJ, Daamen WF, van Kuppevelt TH, Vermes I, Feijen J. First steps towards tissue engineering of small-diameter blood vessels: preparation of flat scaffolds of collagen and elastin by means of freeze drying. *J Biomed Mater Res B Appl Biomater* 2006;77(2):357-68.
68. Tu R, Shen SH, Lin D, Hata C, Thyagarajan K, Noishiki Y, Quijano RC. Fixation of bioprosthetic tissues with monofunctional and multifunctional polyepoxy compounds. *J Biomed Mater Res* 1994;28(6):677-84.
69. Wang E, Thyagarajan K, Tu R, Lin D, Hata C, Shen SH, Quijano RC. Evaluation of collagen modification and surface properties of a bovine artery via polyepoxy compound fixation. *Int J Artif Organs* 1993;16(7):530-6.
70. Gurnani S, Arifuddin M. Effect of visible light on amino acids. II. Histidine. *Photochem Photobiol* 1966;5(4):341-5.
71. Gurnani S, Arifuddin M, Augusti KT. Effect of visible light on amino acids. I. Tryptophan. *Photochem Photobiol* 1966;5(7):495-505.
72. Schmidt CE, Baier JM. Acellular vascular tissues: natural biomaterials for tissue repair and tissue engineering. *Biomaterials* 2000;21(22):2215-31.
73. Bianco RW, Phillips R, Mrachek J, Witson J. Feasibility evaluation of a new pericardial bioprosthesis with dye mediated photo-oxidized bovine pericardial tissue. *J Heart Valve Dis* 1996;5(3):317-22.
74. Moore MA, Adams AK. Calcification resistance, biostability, and low immunogenic potential of porcine heart valves modified by dye-mediated photooxidation. *J Biomed Mater Res* 2001;56(1):24-30.
75. Broderick EP, O'Halloran DM, Rochev YA, Griffin M, Collighan RJ, Pandit AS. Enzymatic stabilization of gelatin-based scaffolds. *J Biomed Mater Res B Appl Biomater* 2005;72(1):37-42.
76. Folk JE. Transglutaminases. *Annu Rev Biochem* 1980;49:517-31.
77. Yokoyama K, Nio N, Kikuchi Y. Properties and applications of microbial transglutaminase. *Appl Microbiol Biotechnol* 2004;64(4):447-54.
78. Chen RN, Ho HO, Sheu MT. Characterization of collagen matrices crosslinked using microbial transglutaminase. *Biomaterials* 2005;26(20):4229-35.
79. O Halloran DM, Collighan RJ, Griffin M, Pandit AS. Characterization of a microbial transglutaminase cross-linked type II collagen scaffold. *Tissue Eng* 2006;12(6):1467-74.
80. Curcio CA, Commerford PJ, Rose AG, Stevens JE, Barnard MS. Calcification of glutaraldehyde-preserved porcine xenografts in young patients. *J Thorac Cardiovasc Surg* 1981;81(4):621-5.
81. Viguet-Carrin S, Garnero P, Delmas PD. The role of collagen in bone strength. *Osteoporos Int* 2006;17(3):319-36.
82. Ottani V, Raspanti M, Ruggeri A. Collagen structure and functional implications. *Micron* 2001;32(3):251-60.
83. Freytes DO, Rundell AE, Vande Geest J, Vorp DA, Webster TJ, Badylak SF. Analytically derived material properties of multilaminated extracellular matrix devices using the ball-burst test. *Biomaterials* 2005;26(27):5518-31.
84. Yahia LH, Drouin G. Study of the hysteresis phenomenon in canine anterior cruciate ligaments. *J Biomed Eng* 1990;12(1):57-62.
85. Billiar KL, Throm AM, Frey MT. Biaxial failure properties of planar living tissue equivalents. *J Biomed Mater Res A* 2005;73(2):182-91.
86. Treloar L. *The Physics of Rubber Elasticity*. London: Oxford University Press; 1975. 1297-1305 p.

87. Billiar KL, Sacks MS. Biaxial mechanical properties of the natural and glutaraldehyde treated aortic valve cusp--Part I: Experimental results. *J Biomech Eng* 2000;122(1):23-30.
88. Rivlin R, Saunders D. Large elastic deformations of isotropic materials, VII. *Philos. Trans. R. Soc.* 1951;A243:251-88.
89. Lanir Y, Fung YC. Two-dimensional mechanical properties of rabbit skin. I. Experimental system. *J Biomech* 1974;7(1):29-34.
90. Lanir Y, Fung YC. Two-dimensional mechanical properties of rabbit skin. II. Experimental results. *J Biomech* 1974;7(2):171-82.
91. Waldman SD, Lee JM. Effect of sample geometry on the apparent biaxial mechanical behaviour of planar connective tissues. *Biomaterials* 2005;26(35):7504-13.
92. Sacks MS, Sun W. Multiaxial mechanical behavior of biological materials. *Annu Rev Biomed Eng* 2003;5:251-84.
93. Sacks MS, Gloeckner DC. Quantification of the fiber architecture and biaxial mechanical behavior of porcine intestinal submucosa. *J Biomed Mater Res* 1999;46(1):1-10.
94. Wasserman AJ, Doillon CJ, Glasgold AI, Kato YP, Christiansen D, Rizvi A, Wong E, Goldstein J, Silver FH. Clinical applications of electron microscopy in the analysis of collagenous biomaterials. *Scanning Microsc* 1988;2(3):1635-46.
95. Fackler K, Klein L, Hiltner A. Polarizing light microscopy of intestine and its relationship to mechanical behaviour. *J Microsc* 1981;124(Pt 3):305-11.
96. Choi HS, Vito RP. Two-dimensional stress-strain relationship for canine pericardium. *J Biomech Eng* 1990;112(2):153-9.
97. Yin FC, Strumpf RK, Chew PH, Zeger SL. Quantification of the mechanical properties of noncontracting canine myocardium under simultaneous biaxial loading. *J Biomech* 1987;20(6):577-89.
98. Chew PH, Yin FC, Zeger SL. Biaxial Stress-strain Properties of Canine Pericardium. *J Mol Cell Cardiol* 1986;18:567-578.
99. Yin FC, Chew PH, Zeger SL. An approach to quantification of biaxial tissue stress-strain data. *J Biomech* 1986;19(1):27-37.
100. Kronick PL, Sacks MS. Quantification of vertical-fiber defect in cattle hide by small-angle light scattering. *Connect Tissue Res* 1991;27(1):1-13.
101. Kronick PL, Buechler PR. Fiber orientation in calf skin by laser light scattering or X-ray diffraction and quantitative relation to mechanical properties. *J Am Leather Chem Assoc* 1986;81:221-229.
102. Hilbert SL, Sword LC, Batchelder KF, Barrick MK, Ferrans VJ. Simultaneous assessment of bioprosthetic heart valve biomechanical properties and collagen crimp length. *J Biomed Mater Res* 1996;31(4):503-9.
103. Birefringence. *AccessScience @ McGraw-Hill: the online encyclopedia of science & technology.* Online ed. New York, NY: Mcgraw-Hill Companies; 2006.
104. Geday MA, Kaminsky W, Lewis JG, Glazer AM. Images of absolute retardance L.Deltan, using the rotating polariser method. *J Microsc* 2000;198 (Pt 1):1-9.
105. Tower TT, Neidert MR, Tranquillo RT. Fiber alignment imaging during mechanical testing of soft tissues. *Ann Biomed Eng* 2002;30(10):1221-33.
106. Bonet J, Wood R. *Nonlinear Continuum Mechanics for Finite Element Analysis.* New York: Cambridge University Press; 1997.
107. Tong P, Fung YC. The stress-strain relationship for the skin. *J Biomech* 1976;9(10):649-57.
108. Hildebrandt J, Fukaya H, Martin CJ. Stress-strain relations of tissue sheets undergoing uniform two-dimensional stretch. *J Appl Physiol* 1969;27(5):758-62.
109. Hoffman AH, Grigg P. A method for measuring strains in soft tissue. *J Biomech* 1984;17(10):795-800.